Corrections to memo 400

Frédéric Boone

February 21, 2002

Some of the input parameters used for the optimization of the ALMA configurations presented in memo 400 were improperly adjusted. As mentioned in the memo the design that was proposed resulted from the application of an analysis and an optimization method. If for some reasons the input parameters were to be changed the resulting design would be different. Since the publication of the memo it was realized that some parameters should be changed because they were based on a wrong reasoning or a wrong interpretation of the PDR recommendations. Here a new design is shown resulting from the application of the same analysis and the same optimization method but with different input parameters.

The changes are listed below:

access constraint: In memo 400 it was assumed that in the compact configuration each antenna should be attainable with a transporter while the other antennas are still observing. It was assumed that roads of 20 m in width should be able to access each antenna without being overlaped by any of the other dishes. In reality the problem of access is not so critical: some of the antennas may not be attainable directly and the dishes may overlap with the roads provided that the centers of the antennas are out of the roads. Then some W-E roads were designed and then a configuration more compact than that of memo 400 was optimized (see Fig.1).

a compact configuration for low elevations: As pointed out by Holdaway (memo 405) the low elevation sources require an elongated compact configuration. In that purpose a second compact configuration was optimized for sources at 30 deg of elevation (see Fig.2).

center of the compact configuration: It was found more optimal to shift the center of the compact configuration of 100 m toward the East. For this new location the topographic constraints are less restricting.

relative size of the configurations: In memo 400 the sizes of the configurations were increased by a constant increment. This was based on a wrong reasoning and the right answer to the question of the relative sizes of the configurations is that the scale factor between consecutive configuration should be constant. For a largest intermediate configuration of 3 km and a compact configuration of 200 m and 4 intermediate configurations the factor is 1.968.

short spacings: Some of the configurations were lacking short baselines. To force a minimum of short spacing some of the antennas situated at the center of the compact configuration were fixed for all the optimizations. 3 antennas are fixed for the optimization of the first intermediate configuration and 2 antennas for the other configurations.

The total resulting number of pads for the compact and intermediate configurations is of 193. The characteristics of the configurations are summarized in Table 1. The configurations are represented in the figures 1, 2, 4, 5, 6. The beams are shown in the figures 7, 8, 9, 10, 11, 12.

NOTE: like in memo 400 the beams shown are simply the Fourier transforms of the sampling function in which each sample is given a weight as described in memo 400.**The Fourier transforms are not multiplied by any function like the autocorelation of the primary beam.** The nuisance of the far sidelobes is therefore exagerated.

Table 1: Characteristics of the configurations.

config.	largest baseline	FWHM of target dist.	duration of the obs.	sampling α	truncation level	resolution @100 GHz
compact	180 m	160 m	1.9 h	1	15.2 dB	$3.41''$
compact 2	206 m	180 m	2.5 h	1	16 dB	$3.05''$
1rst	393 m	353 m	2.0 h	2	15 dB	$1.55''$
2nd	775 m	694 m	3.9 h	2	15 dB	$0.79''$
3rd	1525 m	1366 m	3.8 h	4	15 dB	$0.40''$
4th	3000 m	2690 m	7.5 h	4	15 dB	$0.20''$

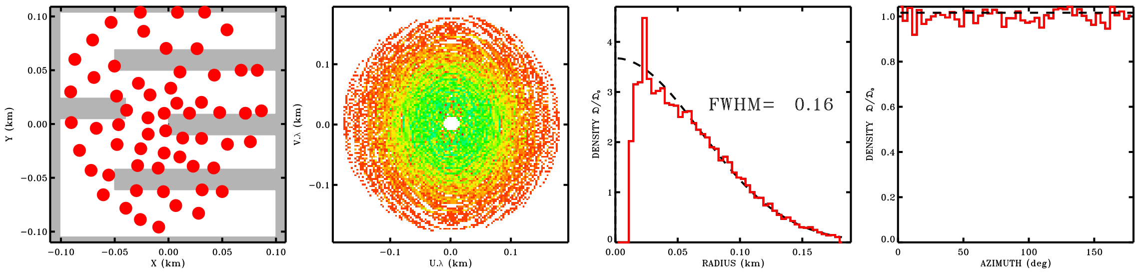

Figure 1: Compact configuration optimized for a Gaussian distribution of visibilities of FWHM= 160 m/λ and a maximum baseline of 180 m (i.e. a truncation level of 15.2 dB) and for the mean source elevation $\epsilon_m = 60\,$deg. The inner boundary condition prevents any shadowing for elevations down to 50 deg.

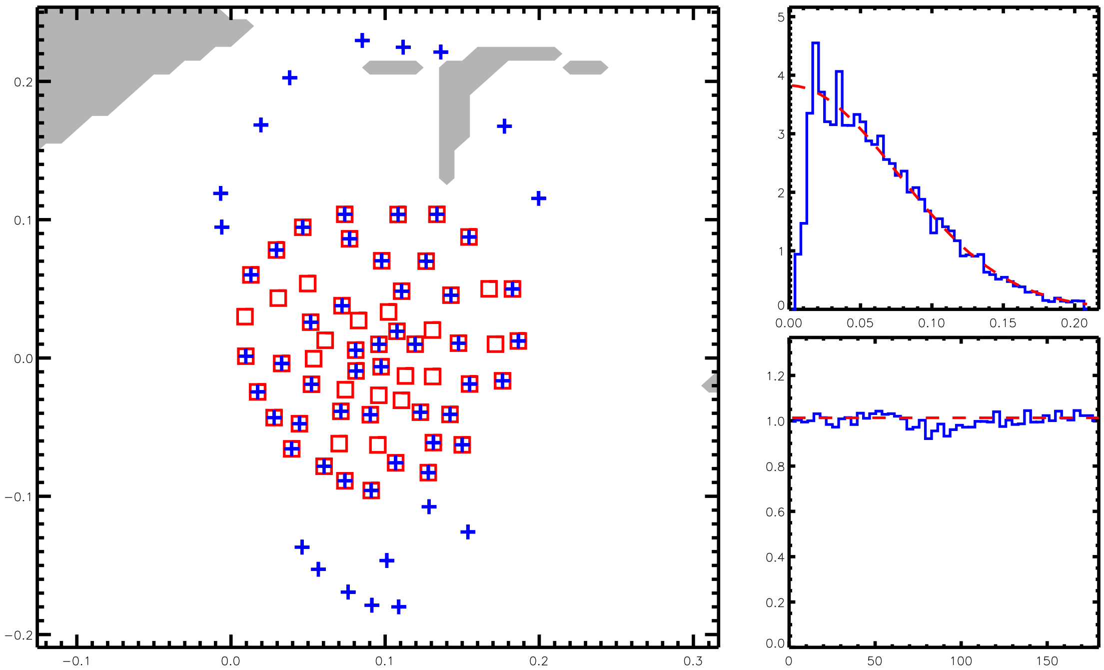

Figure 2: The blue crosses show the locations of the antennas in the second compact configuration optimized for 30 deg of elevation. The red squares show the locations of the pads of the first compact configuration. The figures on the right-hand side show the radial (top) and azimuthal (bottom) distribution of samples.

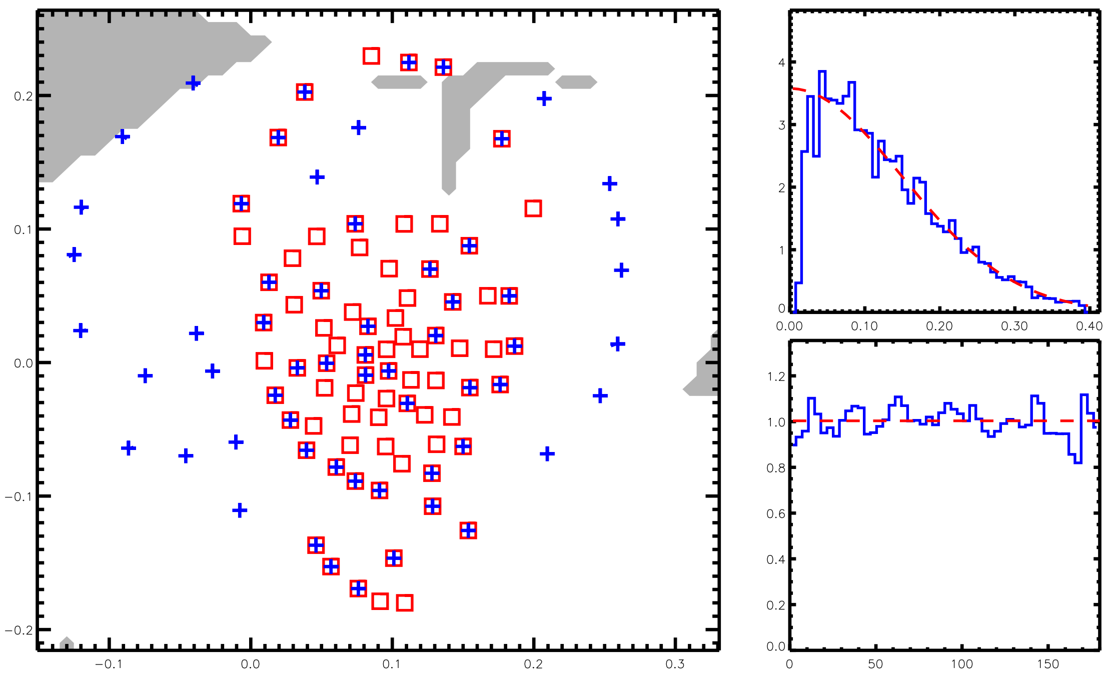

Figure 3: The blue crosses show the locations of the antennas in the first intermediate configuration. The red squares show the locations of the pads of the compact configurations. The figures on the right-hand side show the radial (top) and azimuthal (bottom) distribution of samples.

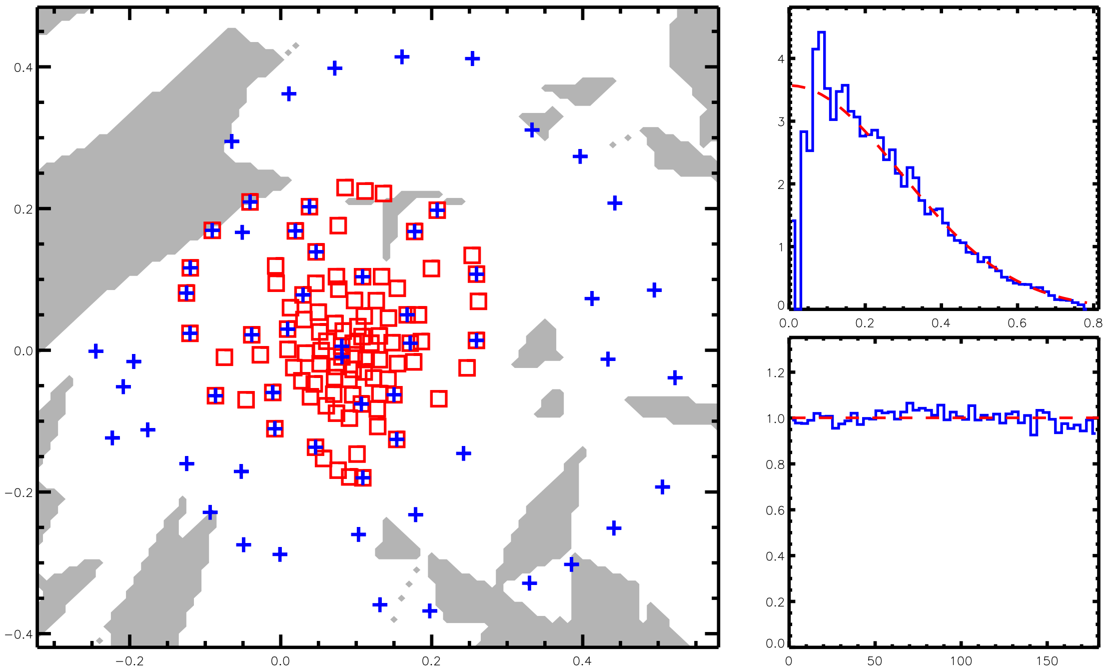

Figure 4: The blue crosses show the locations of the antennas in the second intermediate configuration. The red squares show the locations of the pads of the compact and first intermediate configurations. The figures on the right-hand side show the radial (top) and azimuthal (bottom) distribution of samples.

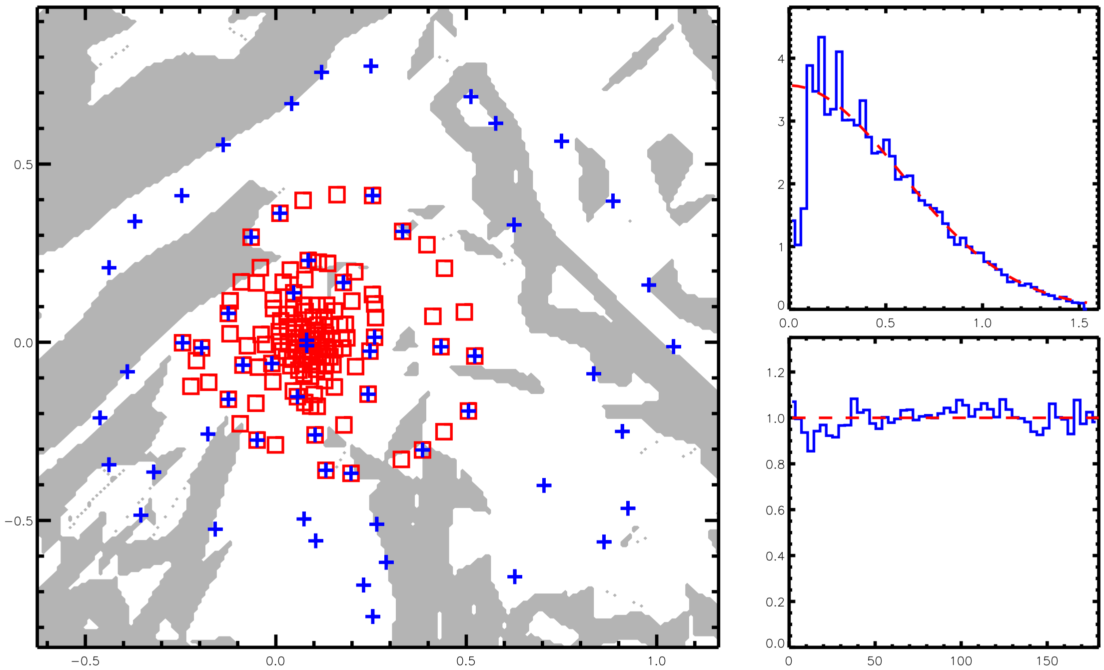

Figure 5: The blue crosses show the locations of the antennas in the third intermediate configuration. The red squares show the locations of the pads of the compact, the first and the second intermediate configurations. The figures on the right-hand side show the radial (top) and azimuthal (bottom) distribution of samples.

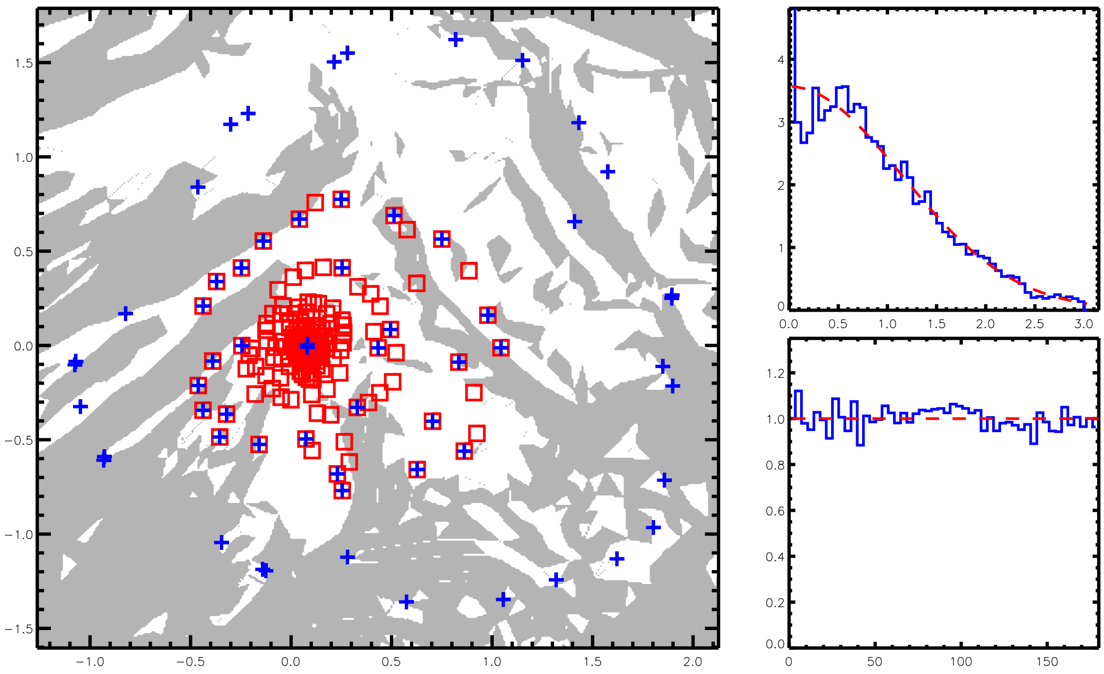

Figure 6: The blue crosses show the locations of the antennas in the fourth intermediate configuration. The red squares show the locations of the pads of the compact and the other intermediate configurations.

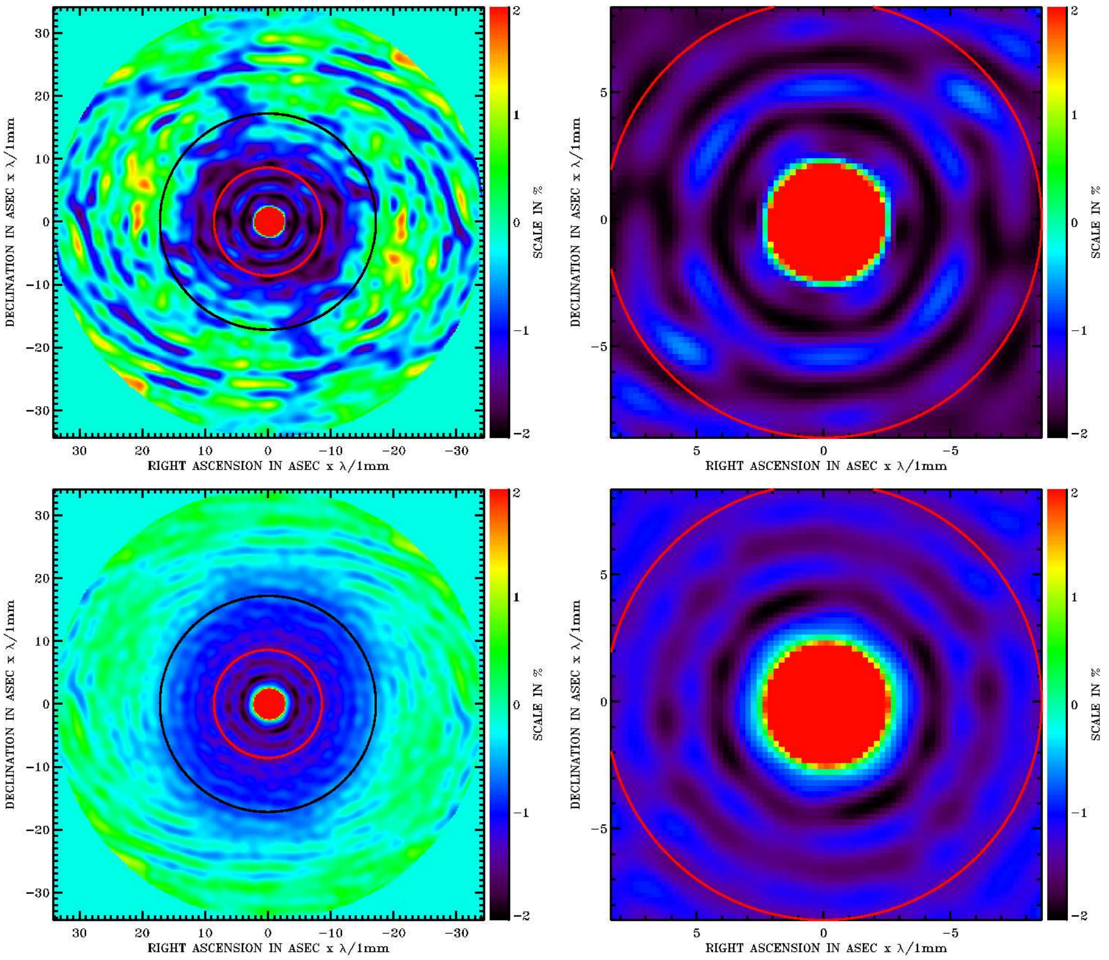

Figure 7: Dirty beam of the first compact configuration using the natural weighting (first row) and a weighting compensating for the excess of density with respect to a perfect Gaussian distribution truncated at 15.2 dB (second row). The loss of sensitivity induced in the latter case is of 2.3%. The red circle represents the half max of the primary beam (assuming FWHM= λ/D) and the black circle represents the field of view (2 FWHM in diameter).

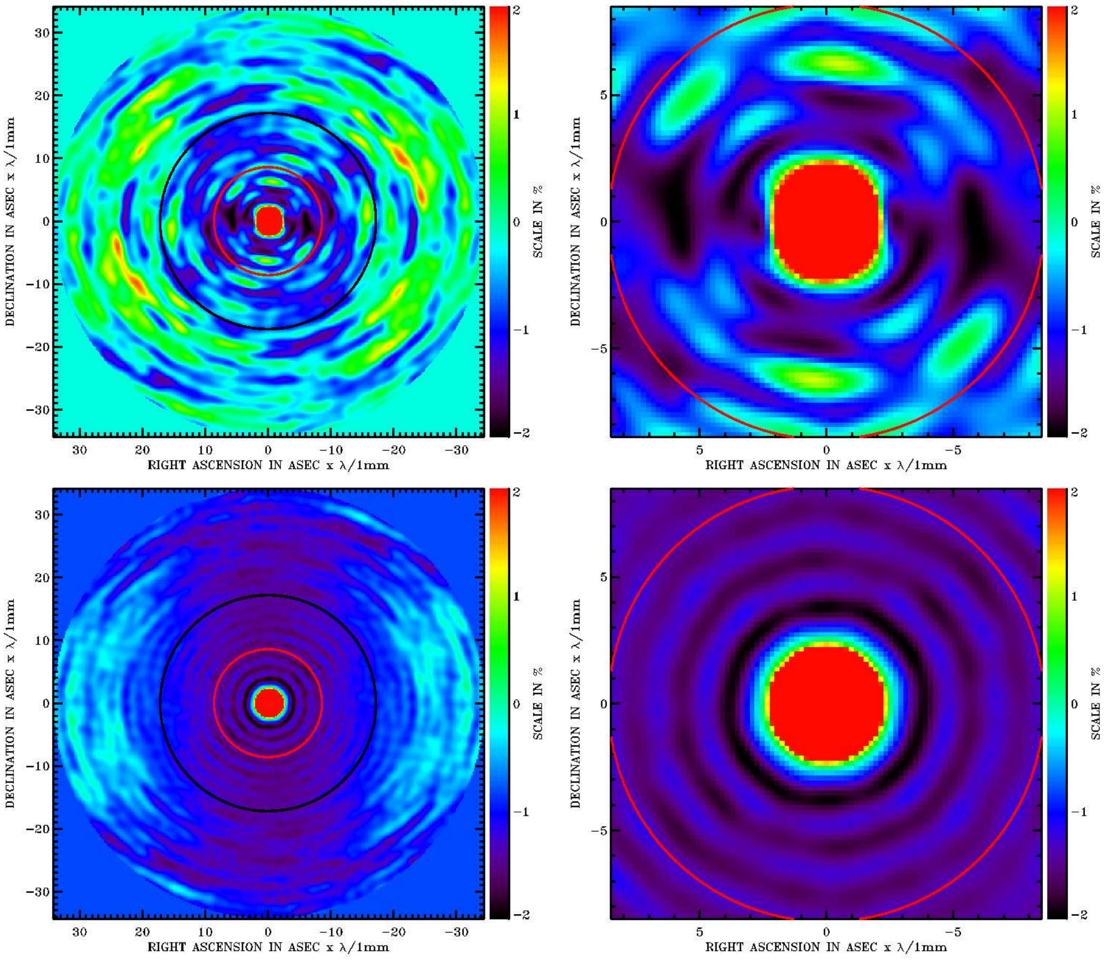

Figure 8: Dirty beam of the second compact configuration using the natural weighting (first row) and a weighting compensating for the excess of density with respect to a perfect Gaussian distribution truncated at 15 dB (second row). The loss of sensitivity induced in the latter case is of 2.8%. The red circle represents the half max of the primary beam (assuming FWHM= λ/D) and the black circle represents the field of view (2 FWHM in diameter).

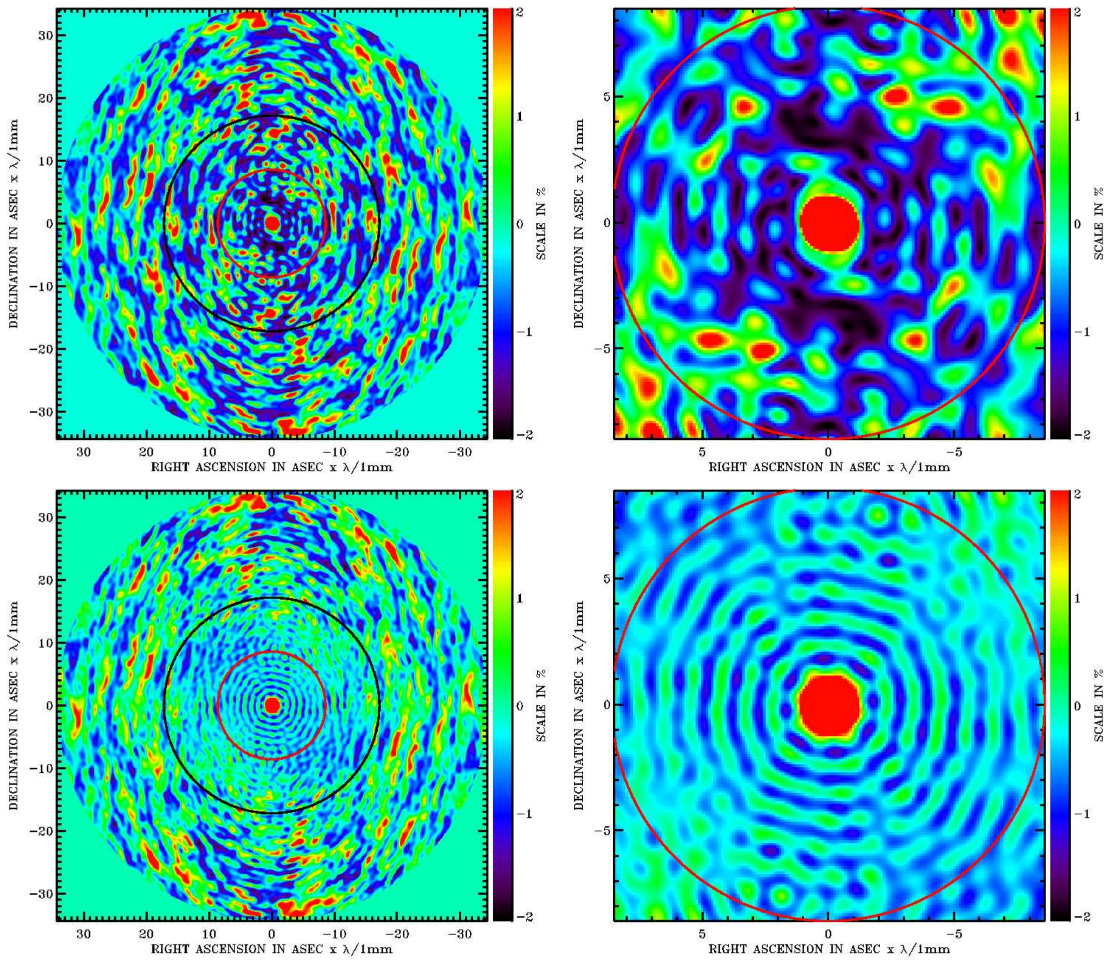

Figure 9: Dirty beam of the first intermediate configuration using the natural weighting (first row) and a weighting compensating for the excess of density with respect to a perfect Gaussian distribution truncated at 15 dB (second row). The loss of sensitivity induced in the latter case is of 5%. The red circle represents the half max of the primary beam (assuming FWHM= λ/D) and the black circle represents the field of view (2 FWHM in diameter).

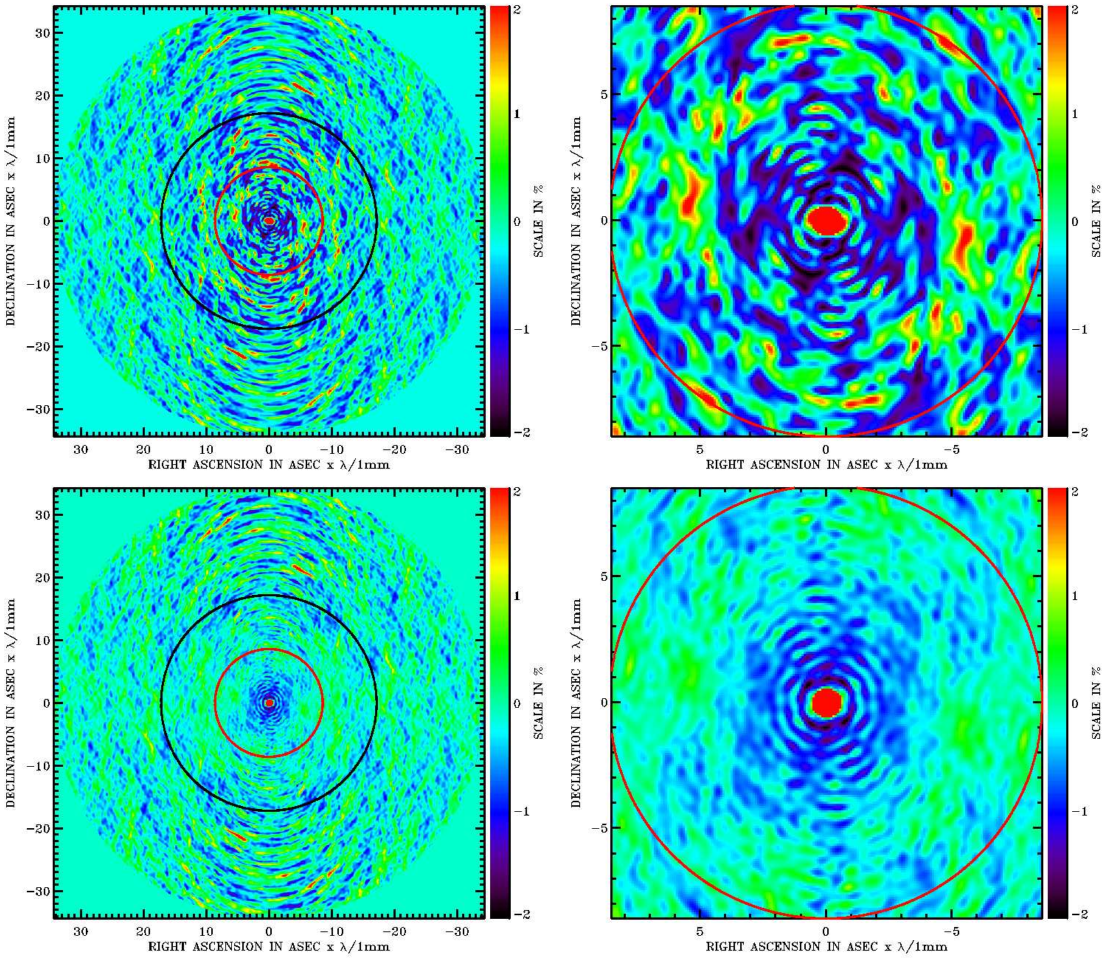

Figure 10: Dirty beam of the second intermediate configuration using the natural weighting (first row) and a weighting compensating for the excess of density with respect to a perfect Gaussian distribution truncated at 15 dB (second row). The loss of sensitivity induced in the latter case is of 5%. The red circle represents the half max of the primary beam (assuming FWHM= λ/D) and the black circle represents the field of view (2 FWHM in diameter).

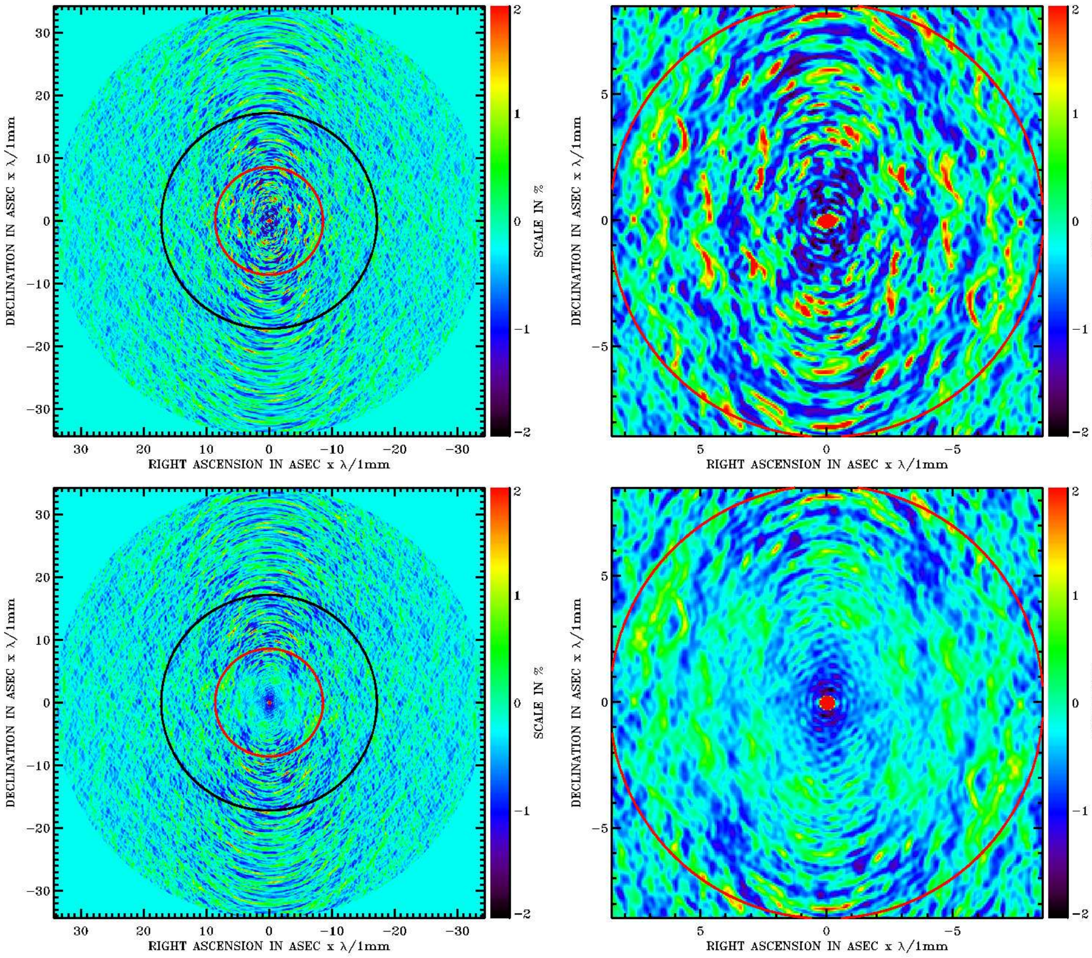

Figure 11: Dirty beam of the third intermediate configuration using the natural weighting (first row) and a weighting compensating for the excess of density with respect to a perfect Gaussian distribution truncated at 15 dB (second row). The loss of sensitivity induced in the latter case is of 5%. The red circle represents the half max of the primary beam (assuming FWHM= λ/D) and the black circle represents the field of view (2 FWHM in diameter).

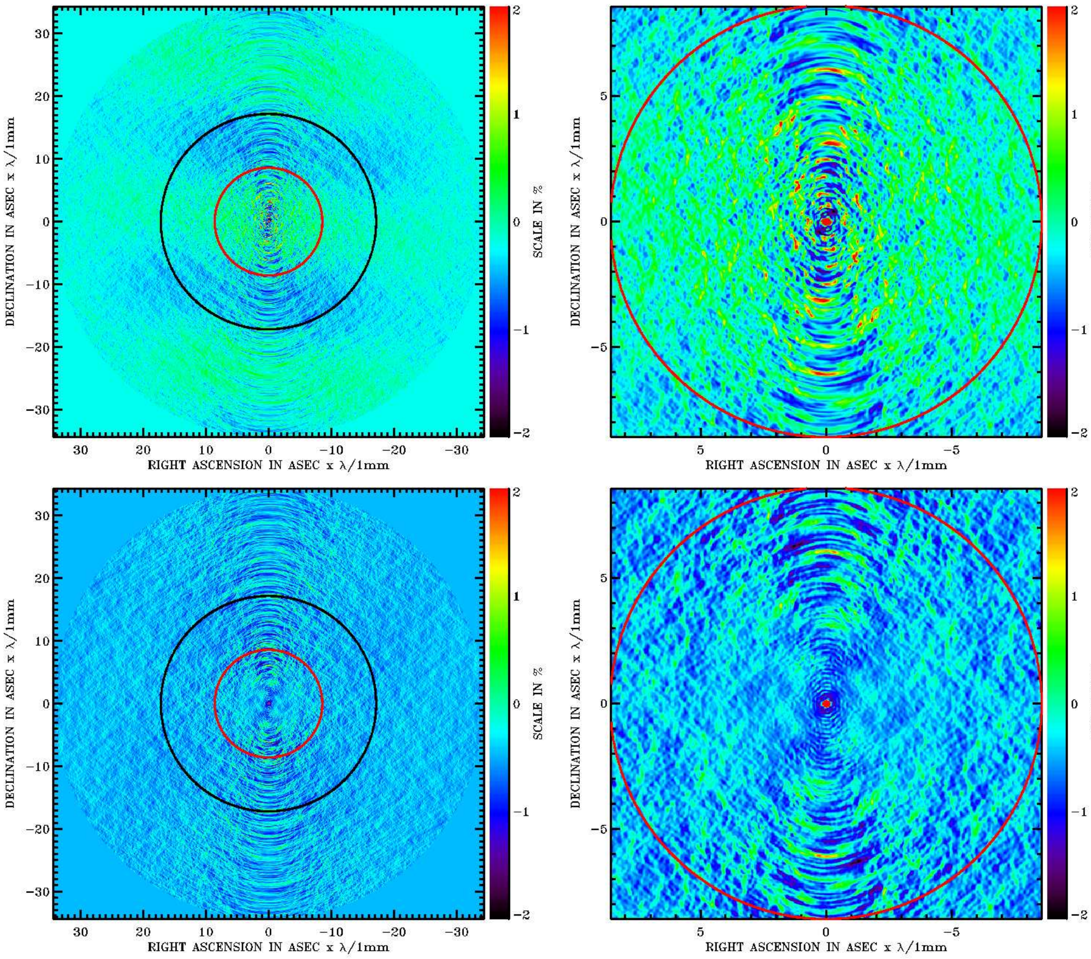

Figure 12: Dirty beam of the fourth intermediate configuration using the natural weighting (first row) and a weighting compensating for the excess of density with respect to a perfect Gaussian distribution truncated at 15 dB (second row). The loss of sensitivity induced in the latter case is of 5%. The red circle represents the half max of the primary beam (assuming FWHM= λ/D) and the black circle represents the field of view (2 FWHM in diameter).